Fundamental Physics Tests by Atom Interferometry

Mark Kasevich
Stanford University
kasevich@stanford.edu

Physical sensitivity limits (10 m apparatus)

Quantum limited accelerometer resolution: ~ 7×10^{-20} g

Assumptions:

1) Wavepackets (Rb) separated by z = 10 m, for T = 1 sec. For 1 g acceleration: $\Delta\phi \sim mgzT/\hbar \sim 1.3 \times 10^{11}$ rad
2) Signal-to-noise for read-out: SNR ~ 10^5:1 per second.
3) Resolution to changes in g per shot: $\delta g \sim 1/(\Delta\phi\ SNR) \sim 7 \times 10^{-17}$ g
4) 10^6 seconds data collection

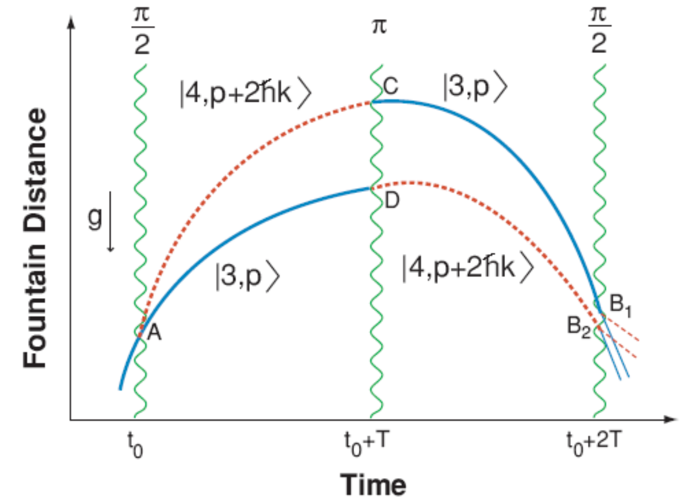

We will exploit this sensitivity for:

Gravity wave detection, tests of General Relativity, new atom charge neutrality tests, tests of QED (photon recoil measurements), searches for anomalous forces…

Equivalence Principle (Ground-based)

Co-falling ^{85}Rb and ^{87}Rb ensembles

Evaporatively cool to enforce tight control over kinematic degrees of freedom

Statistical sensitivity

$\delta g \sim 10^{-15}$ g with 1 month data collection (2 $\hbar$k atom optics)

Systematic uncertainty

$\delta g/g \sim 10^{-16}$ limited by magnetic field inhomogeneities and gravity anomalies.

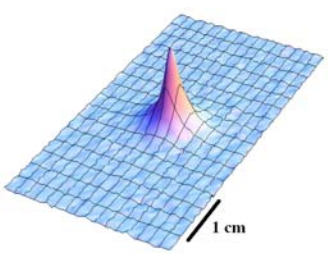

Evaporatively cooled atom source

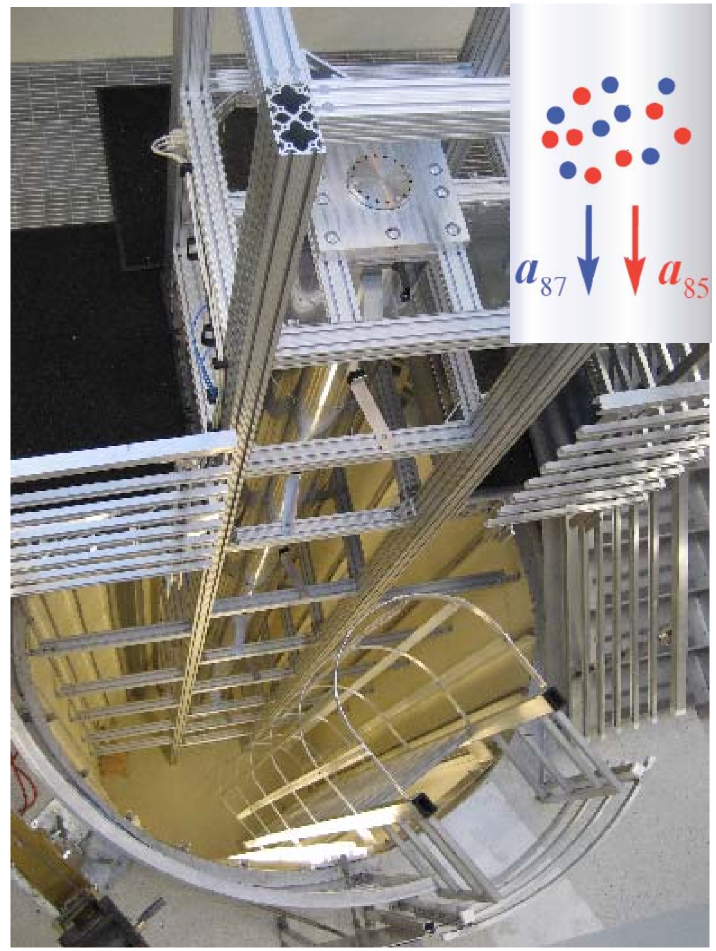

Error Model

Use standard methods to analyze spurious phase shifts from uncontrolled:

- Rotations
- Gravity anomalies/gradients
- Magnetic fields
- Proof-mass overlap
- Misalignments
- Finite pulse effects

Known systematic effects appear controllable at the $\delta g \sim 10^{-16}$ g level.

(Hogan, Johnson, Proc. Enrico Fermi, 2007)

$-k_{eff}\, g\, T^2$	-2.84724×10^{8}	$1.$
$k_{eff}\, R_E\, \Omega_y^2\, T^2$	6.21045×10^{5}	2.18122×10^{-3}
$k_{eff}\, T_{zz}\, V_L\, T^3$	1.57836×10^{3}	5.54347×10^{-6}
$-\frac{7}{12}\, k_{eff}\, T_{zz}\, g\, T^4$	-9.20709×10^{2}	3.23369×10^{-6}
$2\, k_{eff}\, v_{x0}\, \Omega_y\, T^2$	1.97884×10^{1}	6.95002×10^{-8}
$-3\, k_{eff}\, V_L\, \Omega_y^2\, T^3$	-5.16411	1.81373×10^{-8}
$\frac{7}{4}\, k_{eff}\, \Omega_y^2\, g\, T^4$	3.0124	1.05801×10^{-8}
$\frac{7}{12}\, k_{eff}\, R_E\, T_{zz}\, \Omega_y^2\, T^4$	2.00827	7.05338×10^{-9}
$\frac{k_{eff}^2\, T_{zz}\, \hbar\, T^3}{2\, m}$	7.05401×10^{-1}	2.47749×10^{-9}
$k_{eff}\, T_{zz}\, v_{z0}\, T^3$	7.05401×10^{-1}	2.47749×10^{-9}
$k_{eff}\, T_{zz}\, T^2\, z_0$	8.92817×10^{-2}	3.13573×10^{-10}
$-\frac{7}{4}\, k_{eff}\, R_E\, \Omega_y^4\, T^4$	-6.57069×10^{-3}	2.30774×10^{-11}
$-\frac{7}{4}\, k_{eff}\, R_E\, \Omega_y^2\, \Omega_z^2\, T^4$	-3.84744×10^{-3}	1.35129×10^{-11}
$-\frac{3\, k_{eff}^2\, \Omega_y^2\, \hbar\, T^3}{2\, m}$	-2.30795×10^{-3}	8.10592×10^{-12}
$-3\, k_{eff}\, v_{z0}\, \Omega_y^2\, T^3$	-2.30795×10^{-3}	8.10592×10^{-12}
$\frac{1}{4}\, k_{eff}\, T_{zz}^2\, V_L\, T^5$	2.18739×10^{-3}	7.68251×10^{-12}
$3\, k_{eff}\, v_{y0}\, \Omega_y\, \Omega_z\, T^3$	1.76607×10^{-3}	6.20273×10^{-12}
$-\frac{31}{360}\, k_{eff}\, T_{zz}^2\, g\, T^6$	-7.53436×10^{-4}	2.6462×10^{-12}
$4\, B_0\, V_L\, T^2\, \alpha\, b_{z1}$	5.14655×10^{-4}	1.80756×10^{-12}
$-4\, B_0\, g\, T^3\, \alpha\, b_{z1}$	-5.14655×10^{-4}	1.80756×10^{-12}
$k_{eff}\, \Omega_y^2\, T^2\, z_0$	9.73714×10^{-5}	3.41985×10^{-13}
$-k_{eff}\, \Omega_y\, \Omega_z\, T^2\, y_0$	-7.45096×10^{-5}	2.61691×10^{-13}
$\frac{7}{6}\, k_{eff}\, T_{zz}\, v_{x0}\, \Omega_y\, T^4$	6.39894×10^{-5}	2.24742×10^{-13}
$-7\, V_L\, g\, T^4\, \alpha\, b_{z1}^2$	-4.7766×10^{-5}	1.67762×10^{-13}
$\frac{7}{6}\, k_{eff}\, T_{xx}\, v_{x0}\, \Omega_y\, T^4$	-3.19947×10^{-5}	1.12371×10^{-13}
$4\, V_L^2\, T^3\, \alpha\, b_{z1}^2$	2.72948×10^{-5}	9.58642×10^{-14}
$3\, g^2\, T^5\, \alpha\, b_{z1}^2$	2.04711×10^{-5}	7.18982×10^{-14}

Apparatus

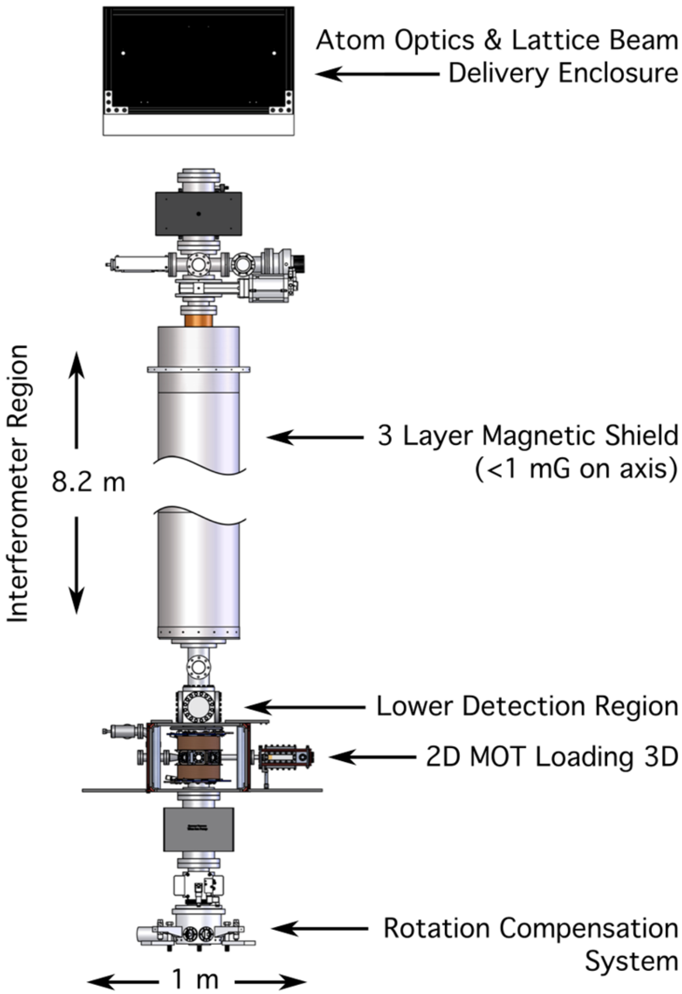

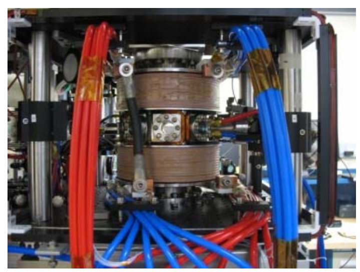

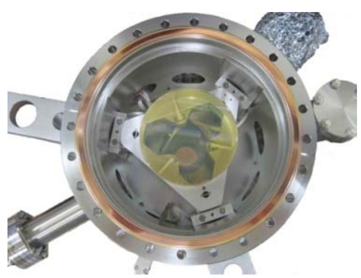

Ultracold atom source

- $>10^6$ atoms at 50 nK
- 3e5 at 3 nK

Optical Lattice Launch

- 13.1 m/s with 2372 photon recoils to 9 m

Atom Interferometry

- 2 cm $1/e^2$ radial waist
- 500 mW total power
- Dynamic nrad control of laser angle with precision piezo-actuated stage

Detection

- Spatially-resolved fluorescence imaging
- Two CCD cameras on perpendicular lines of sight

Current demonstrated statistical resolution, ~5e-13 g in 1 hr (87Rb)

Interference at long interrogation time (T=1.15 s)

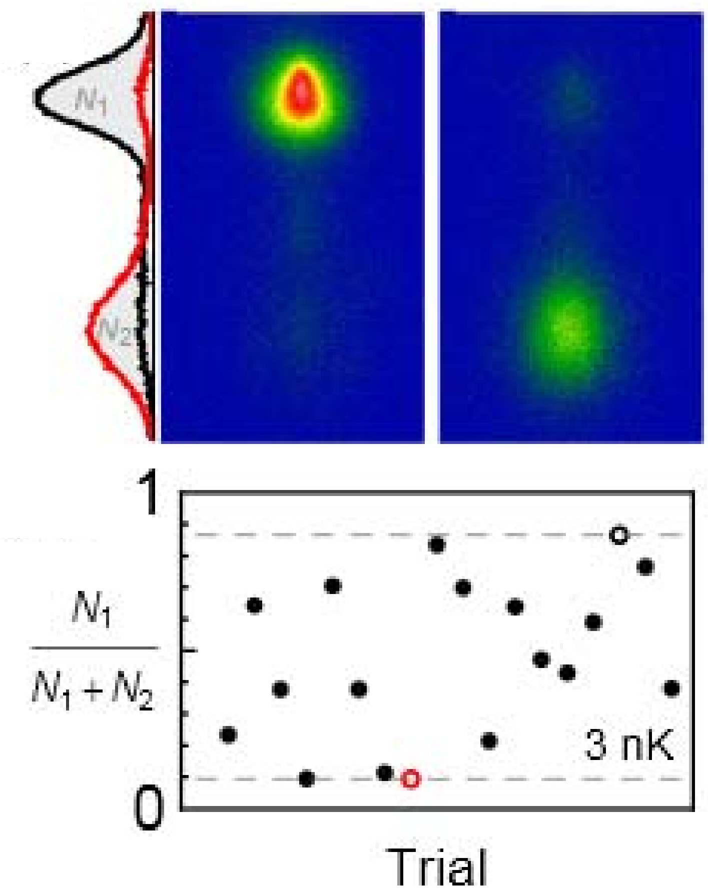

Interference

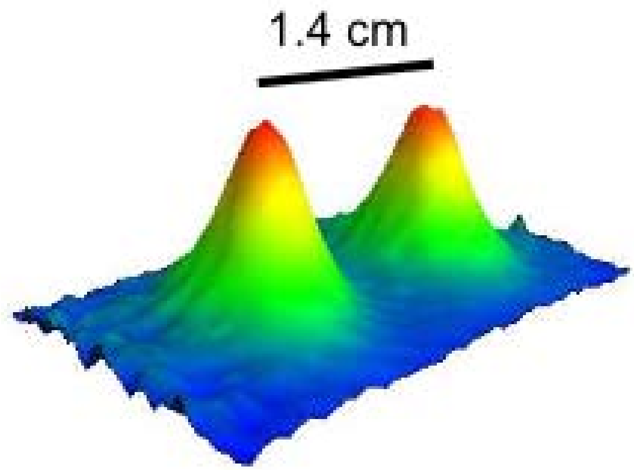

Wavepacket separation at apex

2T = 2.3 sec
Near full contrast
3 nK
6.7e-12 g/shot

Dickerson, et al., arXiv:1305.1700 (2013)

Phase shifts

Term	Phase Shift	Size (rad)	
1	$k_{\text{eff}} g T^2$	2.1×10^8	*Gravity*
2	$2\mathbf{k}_{\text{eff}} \cdot (\mathbf{\Omega} \times \mathbf{v}) T^2$	5.1	*Coriolis*
3	$k_{\text{eff}} v_z \delta T$	3.5	*Timing asymmetry*
4	$\frac{\hbar k_{\text{eff}}^2}{2m} T_{zz} T^3$	0.44	*Curvature, quantum*
5	$k_{\text{eff}} T_{zi} (x_i + v_i T) T^2$	0.18	*Gravity gradient*
6	$\frac{1}{2} k_{\text{eff}} \alpha \left(v_x^2 + v_y^2\right) T^2$	0.04	*Wavefront*

Characterize velocity dependent shifts with spatial imaging
(useful when atoms expand from a point source)

2-axis rotation measurement

Interference patterns for rotating platform:

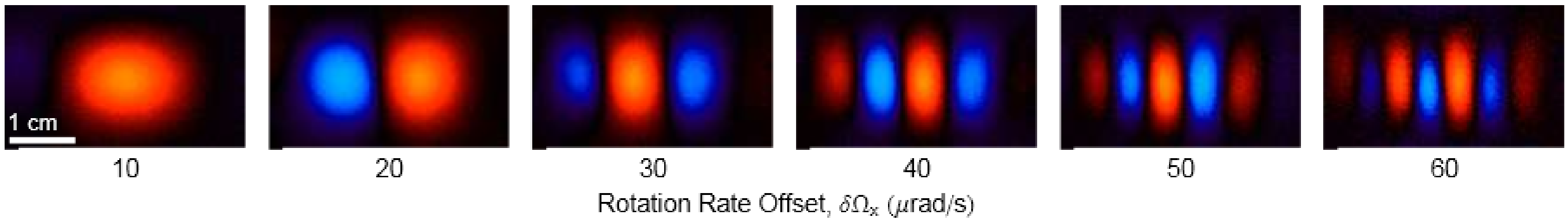

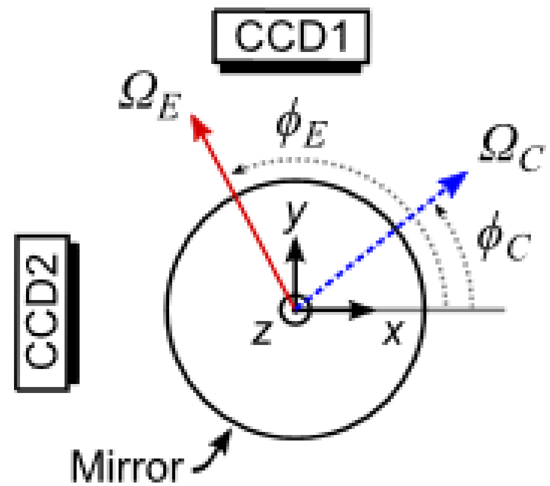

Measurement Geometry

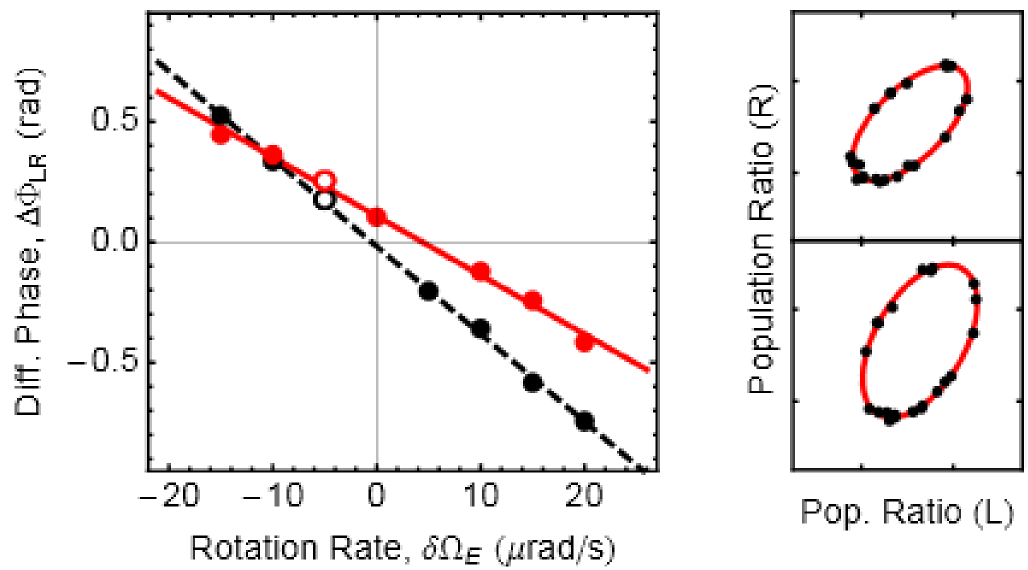

Measurement of rotation rate near null rotation operating point. Other form factors possible!

Dickerson, et al., arXiv:1305.1700 (2013)

Magnetic lens cooling

Use diabatic steps in strength of TOP trap to cool atoms:

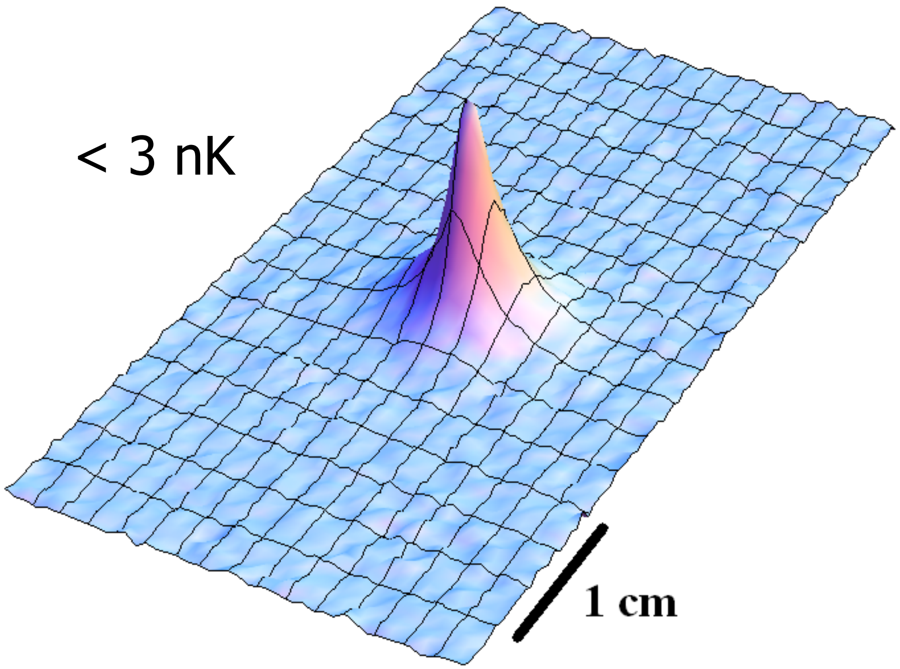

Atom cloud imaged after 2.6 seconds free-fall

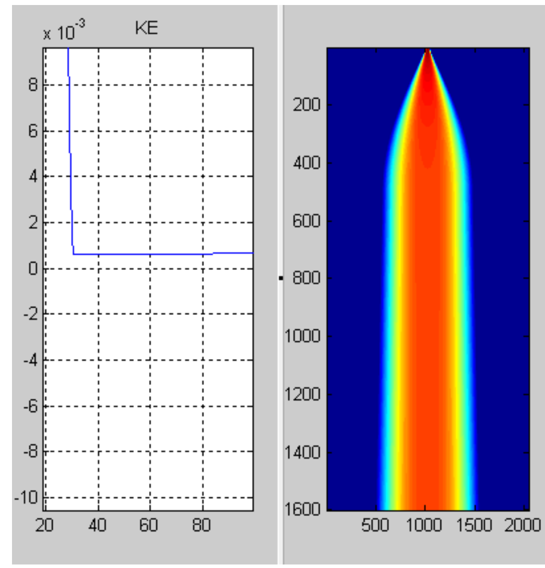

Simulation of microgravity cooling performance.

~1 pK temperatures achievable.

Phase shear readout

Tilt angle of final pulse to introduce a phase shear

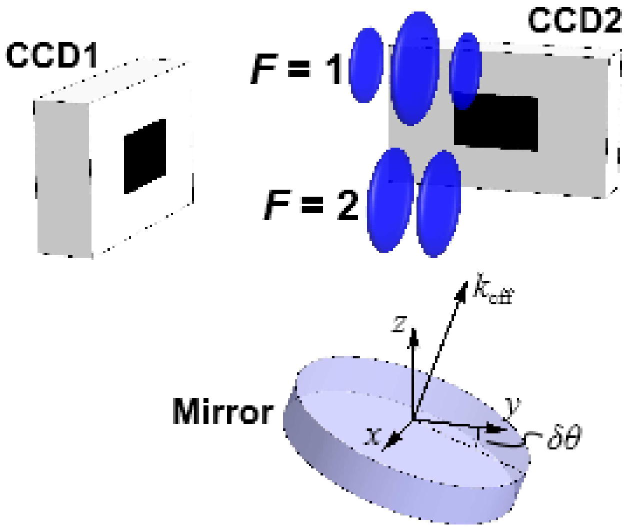

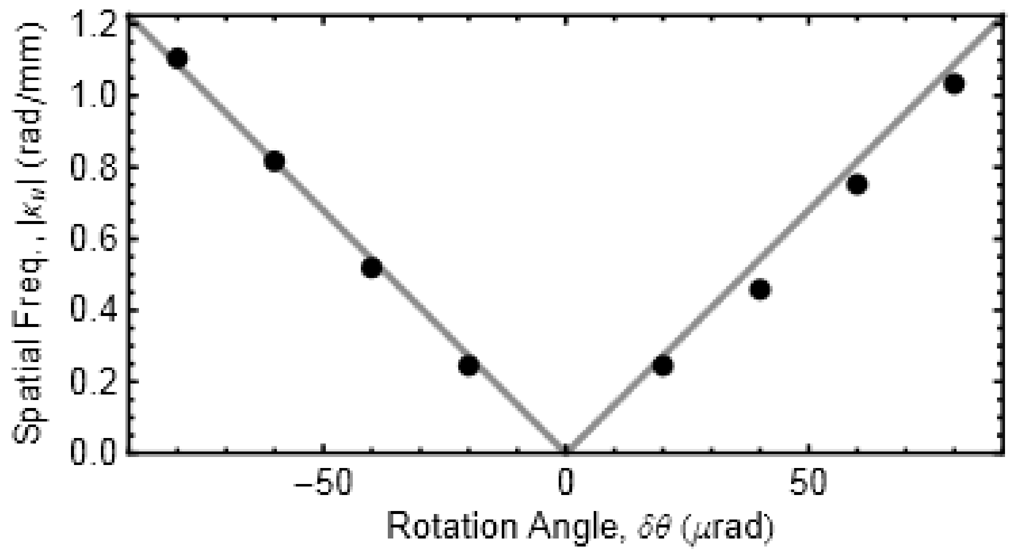

Enables simultaneous read-out of contrast and phase

Sugarbaker, et al., arXiv:1305.3298 (2013).

Phase shear readout

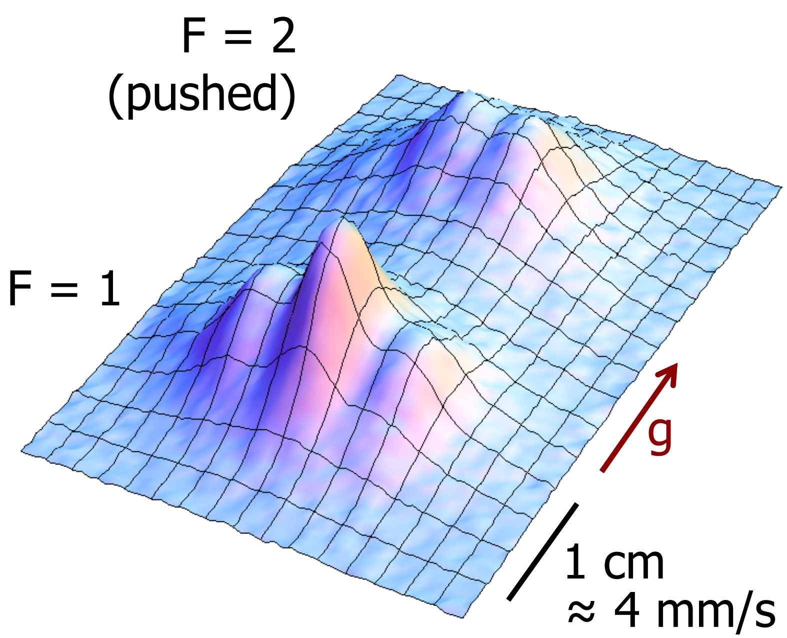

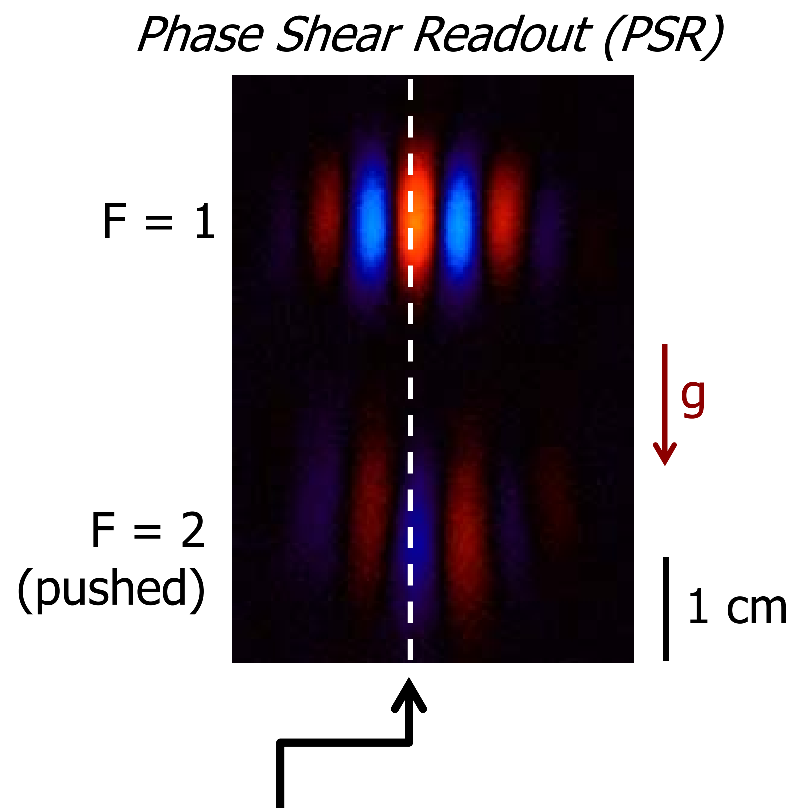

Single-shot interferometer phase measurement

Mitigates noise sources:

✓ Satellite pointing jitter and residual rotation readout

✓ Laser wavefront aberration in situ characterization

Phase shear readout

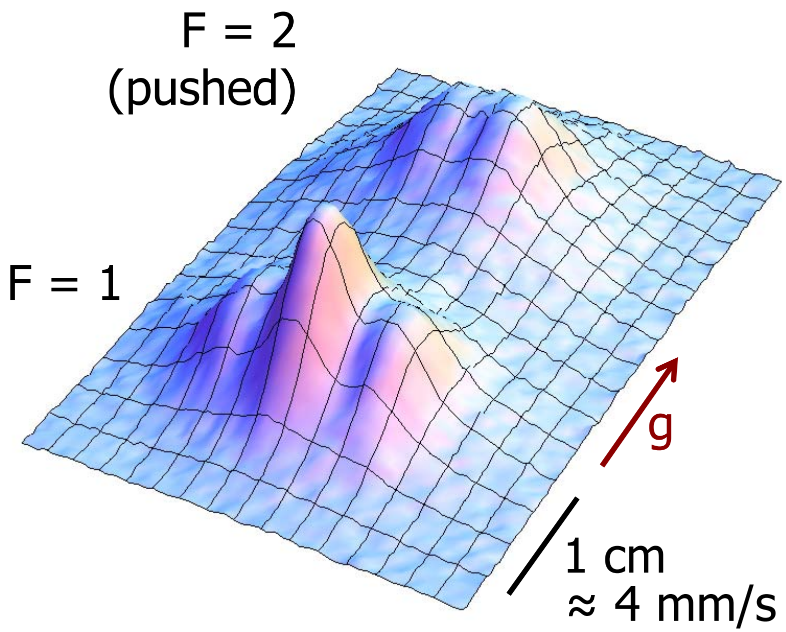

Phase Shear Readout (PSR)

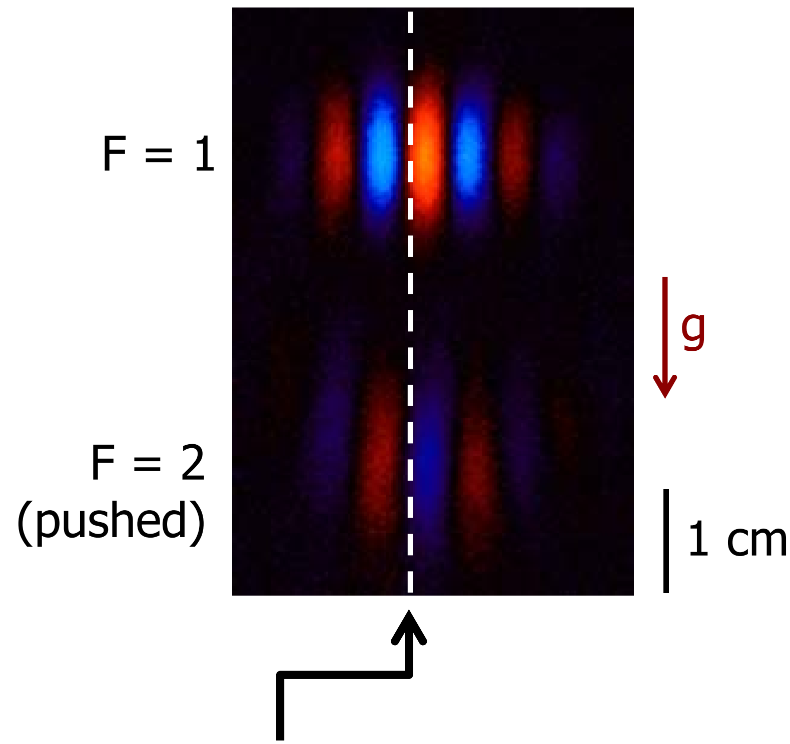

Single-shot interferometer phase measurement

Mitigates noise sources:

✓ Satellite pointing jitter and residual rotation readout

✓ Laser wavefront aberration in situ characterization

Phase shear readout

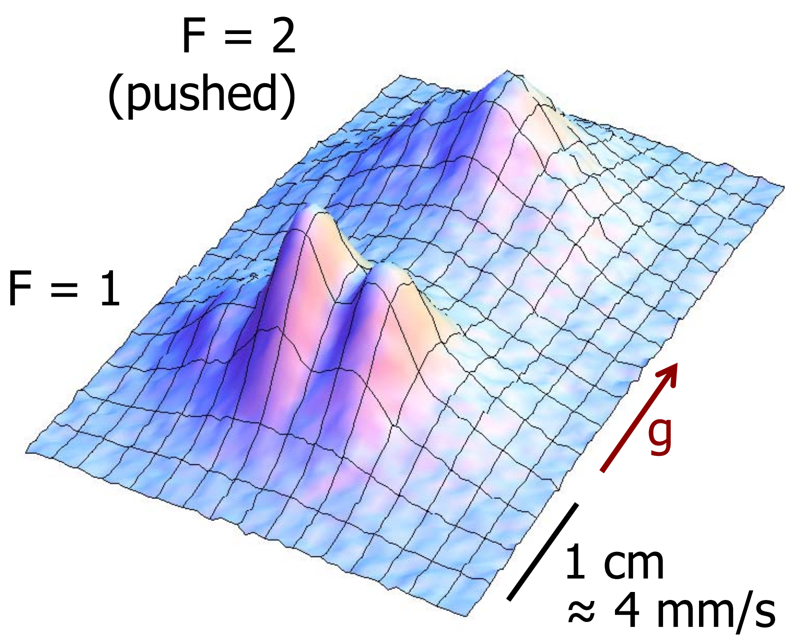

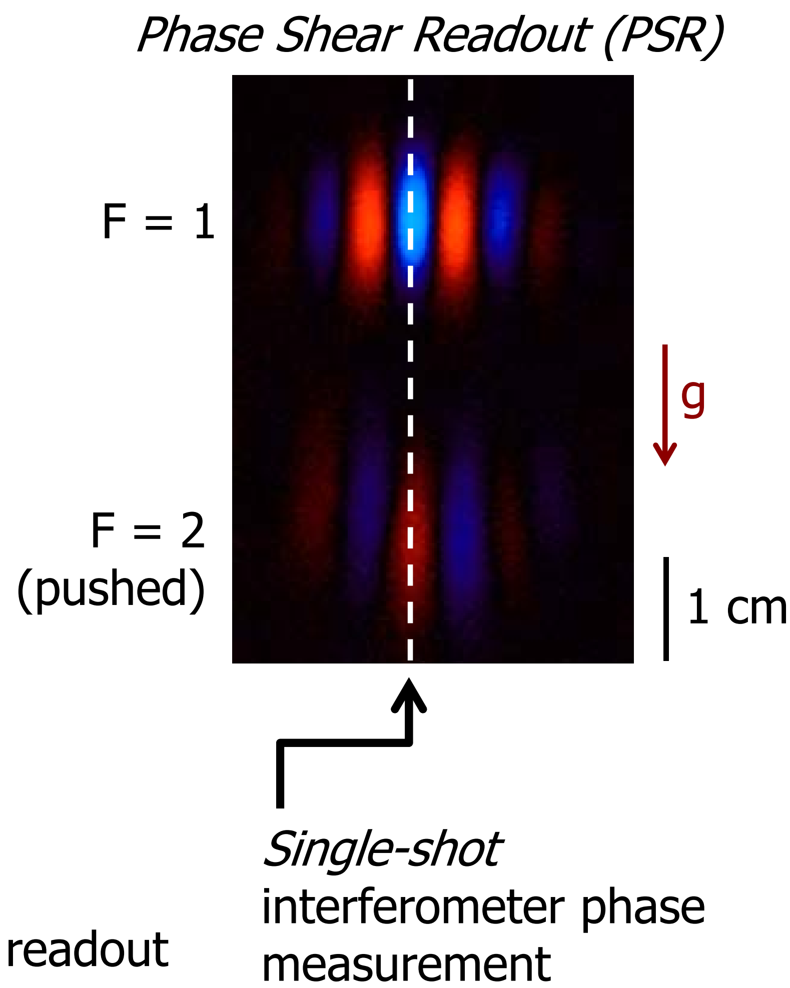

Mitigates noise sources:

✓ Satellite pointing jitter and residual rotation readout

✓ Laser wavefront aberration in situ characterization

Phase shear readout

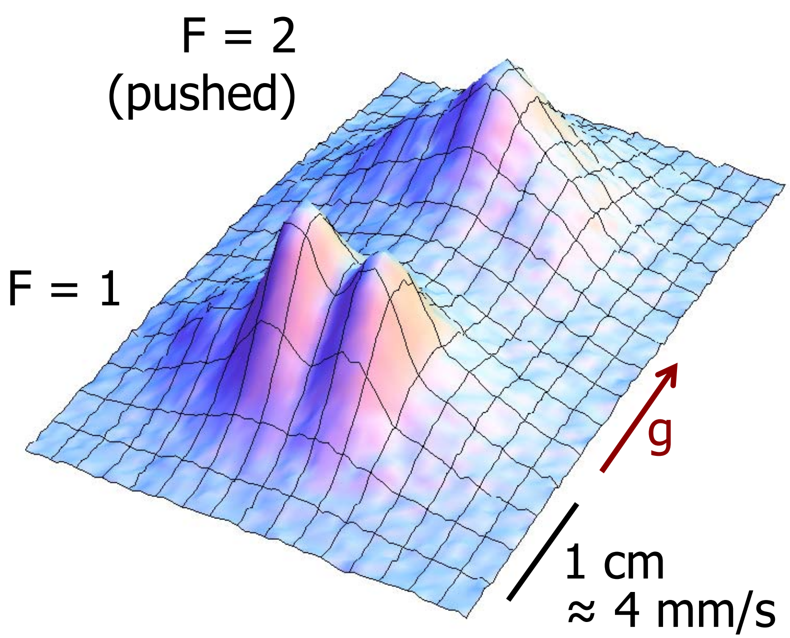

Phase Shear Readout (PSR)

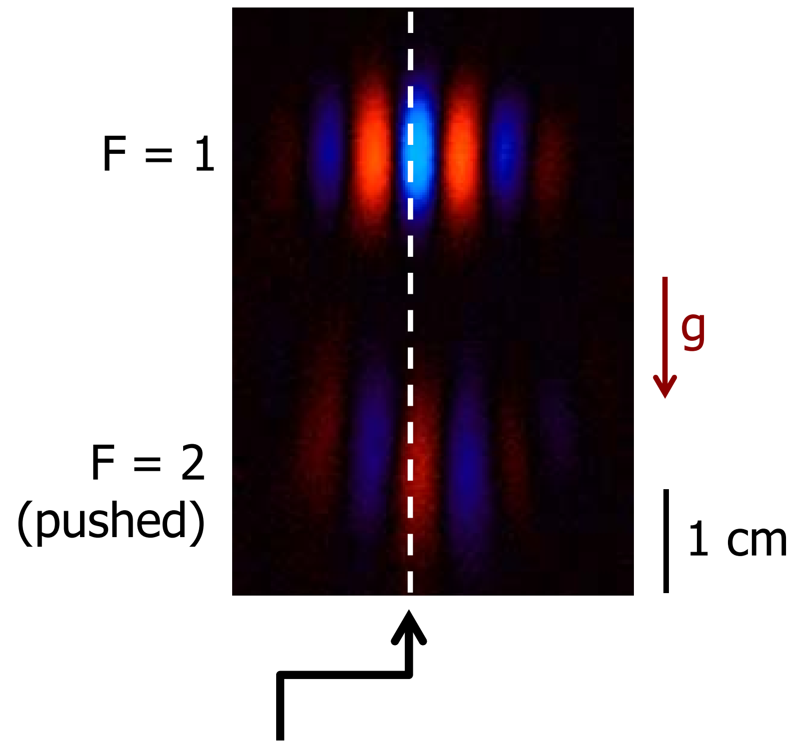

Single-shot interferometer phase measurement

Mitigates noise sources:

- ✓ Satellite pointing jitter and residual rotation readout
- ✓ Laser wavefront aberration in situ characterization

Phase shear/timing asymmetry

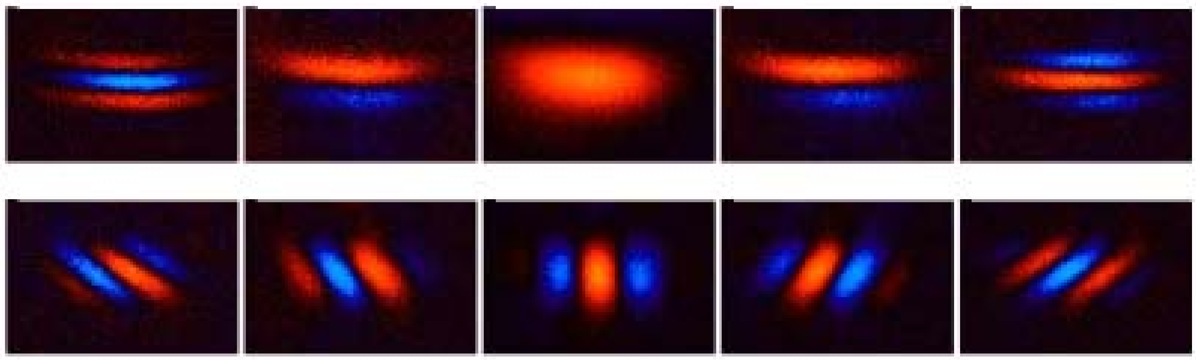

Timing asymmetry

Timing asymmetry + beam tilt

Fringe shear vs. timing asymmetry

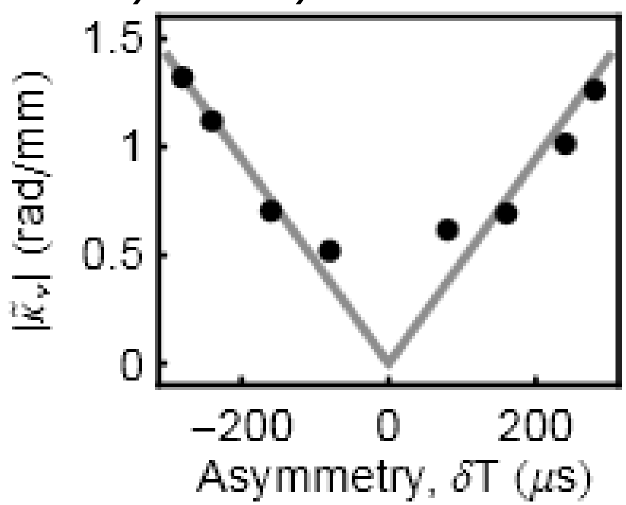

Angle vs. timing asymmetry w/ beam tilt

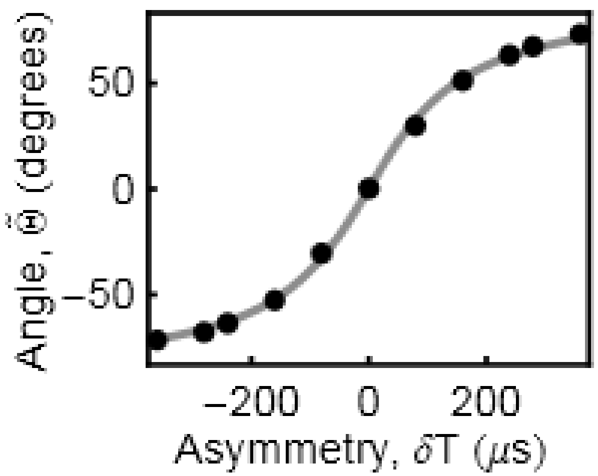

Gyrocompass demonstration using phase shear

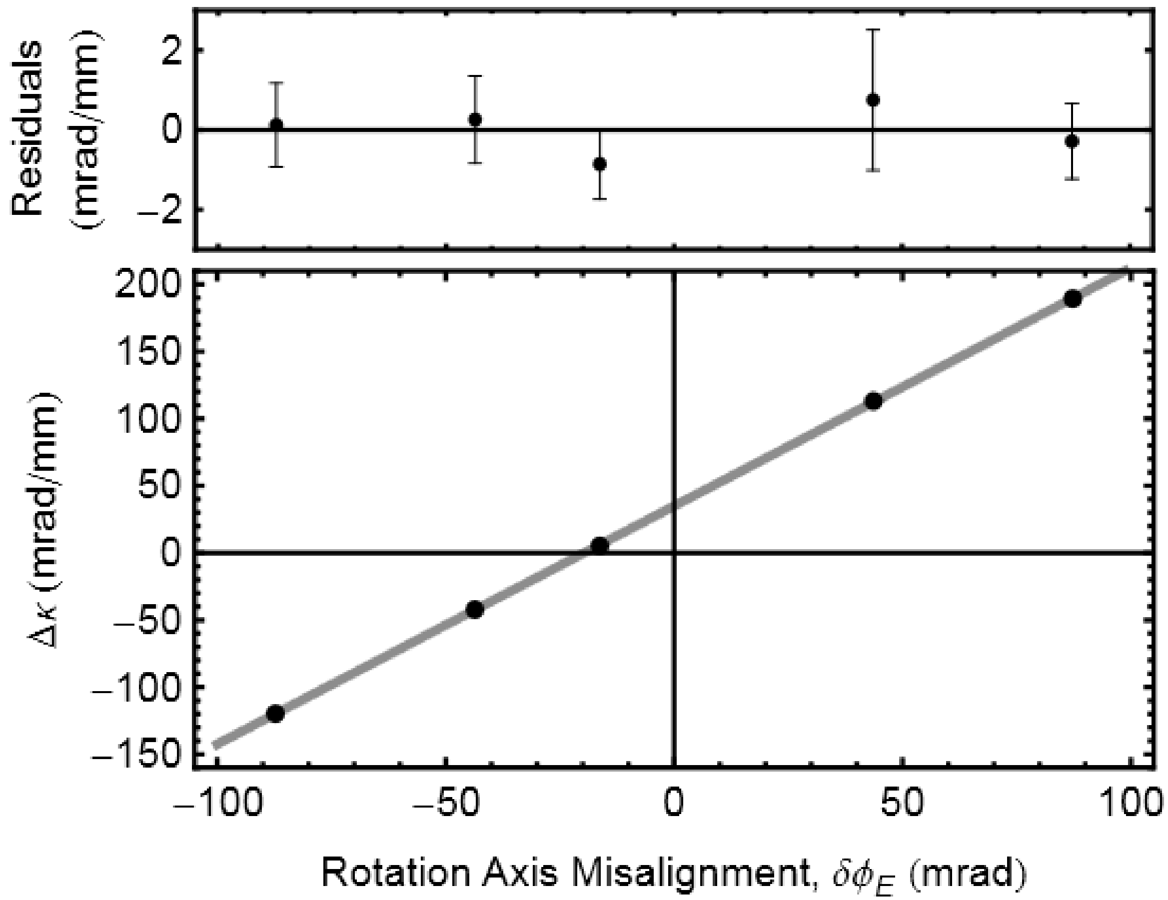

Use phase shear to determine determine true North

Vary rotation compensation direction, measure phase shear

10 mdeg resolution in 1 hr.

Satellite GW Antenna

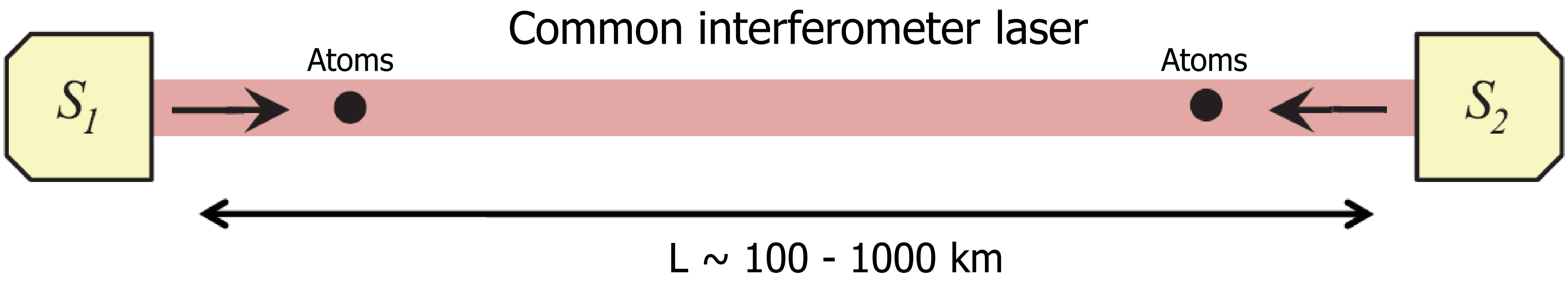

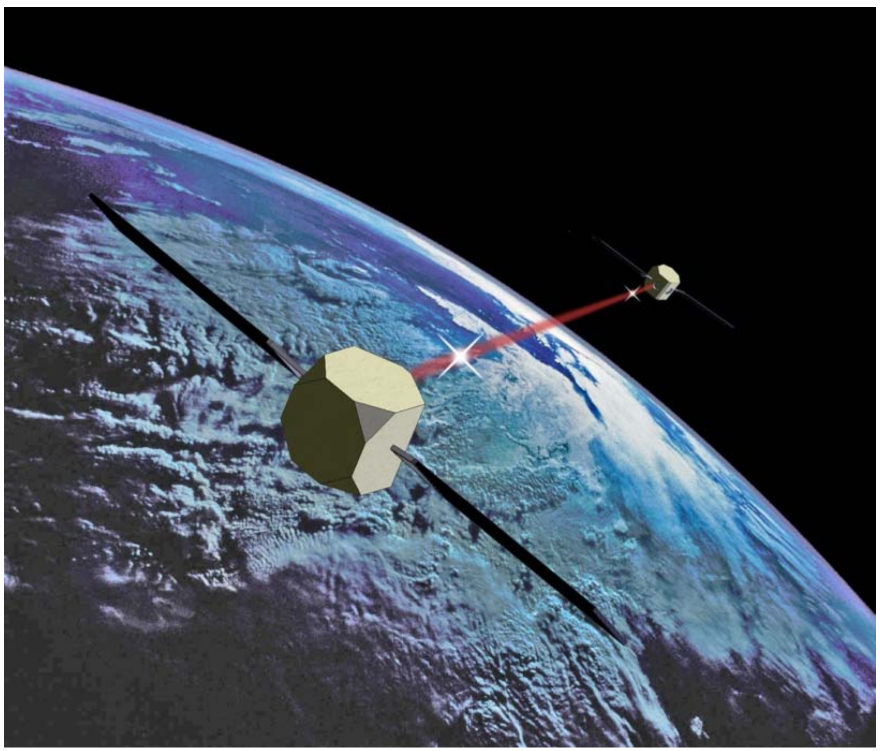

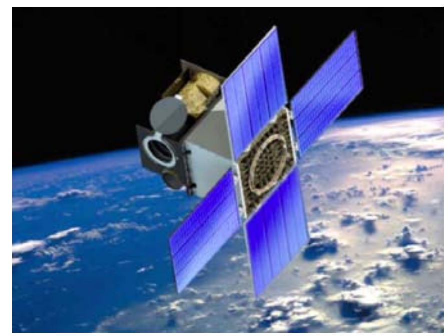

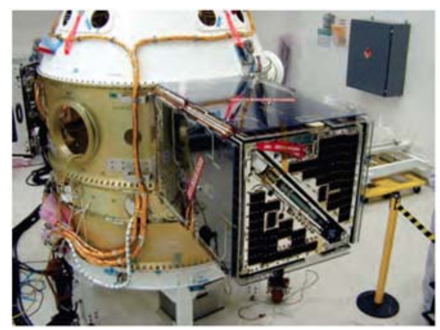

JMAPS bus/ESPA deployed

Potential Strain Sensitivity

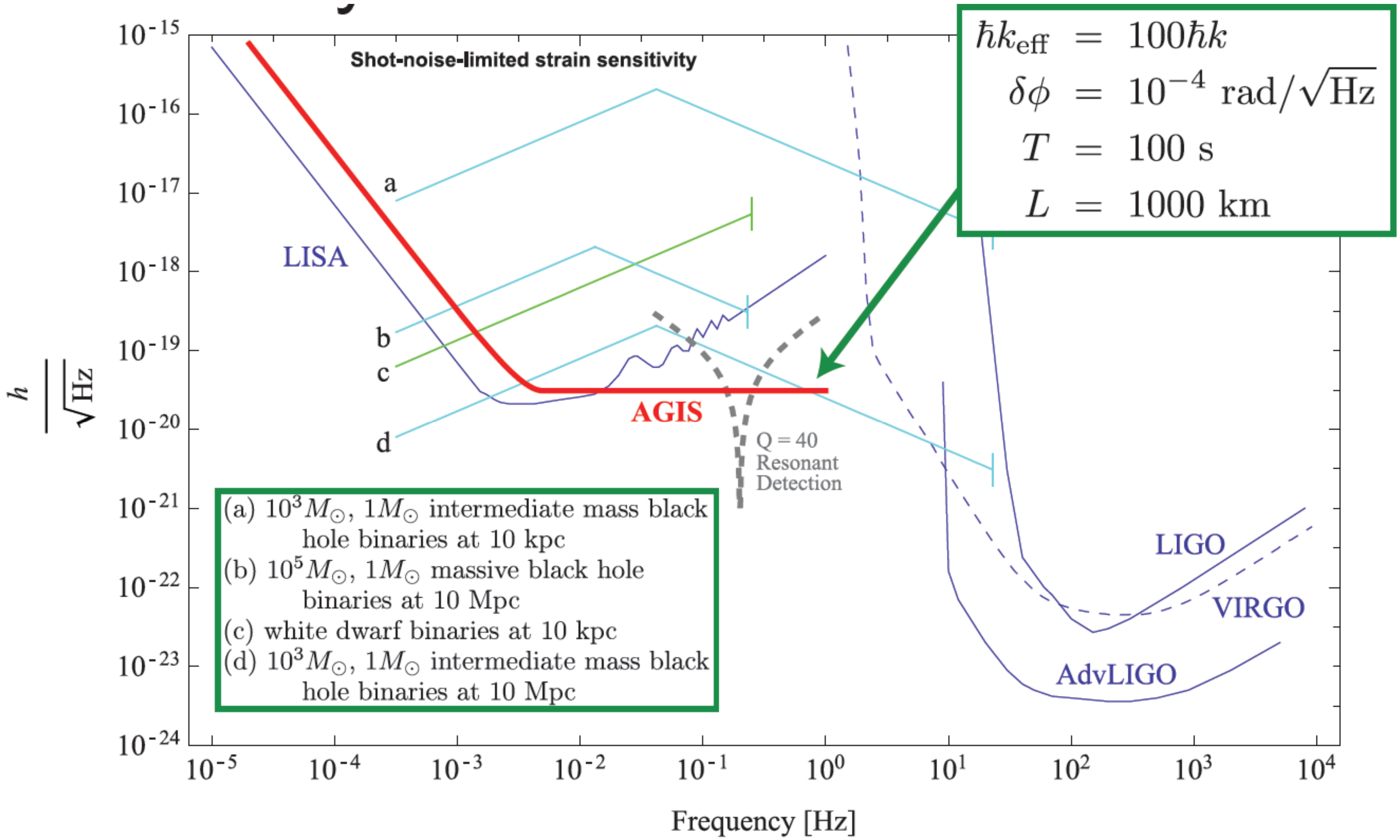

J. Hogan, et al., GRG **43**, 7 (2011).

Analysis details

Curved wavefronts: momentum recoil depends on position in beam.

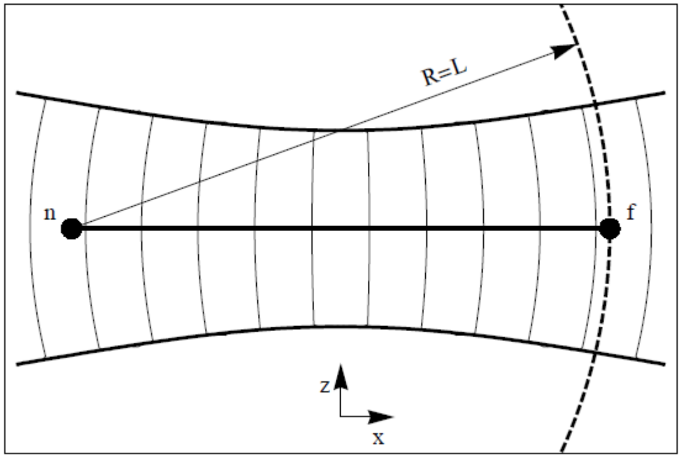

Design pulse sequences to accommodate Coriolis deflections of wavepacket trajectories and laser wavefront curvature.

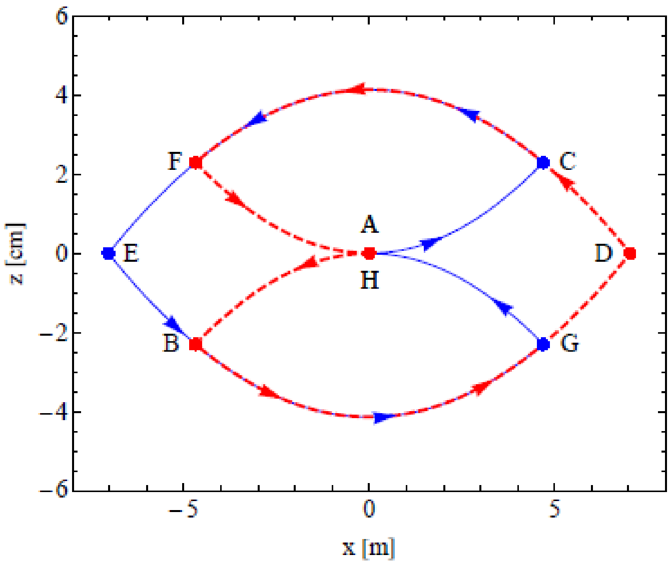

5-pulse football sequence

Error Model

Analysis to determine requirements on satellite jitter, laser pointing stability, atomic source stability, and orbit gravity gradients.

	Differential phase shift	Size (rad)	Constraint
1	$\frac{1485 k_{\mathrm{eff}}^3 \hbar^2}{4Lm^2} T^6 T_{\mathrm{xx}} \Omega_{\mathrm{or}} \delta\Omega$	$(180\ \mathrm{s})\delta\Omega$	$\delta\Omega < 0.57\ \mu\mathrm{rad/s}$
2	$\frac{1485 k_{\mathrm{eff}}^3 \hbar^2}{2Lm^2} T^6 \Omega_{\mathrm{or}}^3 \varepsilon_{zz} \delta\Omega$	$(350\ \mathrm{s})\varepsilon_{zz}\delta\Omega$	$\varepsilon_{zz} < 0.50$
3	$\frac{15}{2} k_{\mathrm{eff}} T^4 R \Omega_{\mathrm{or}}^2 \left(15T\left(T_{zz} + 3\Omega_{\mathrm{or}}^2\right) + 8\Phi\Omega_{\mathrm{or}}\right) \varepsilon_g \delta\Omega$	$(3 \times 10^9\ \mathrm{s})\, \varepsilon_g \delta\Omega$	$\varepsilon_g < 5.8 \times 10^{-8}$
4	$30 k_{\mathrm{eff}} T^4 \Omega_{\mathrm{or}}^4 \varepsilon_{\mathrm{xx}} (\delta x_{\mathrm{n}} - \delta x_{\mathrm{f}})$	$(22\ \mathrm{m}^{-1})\varepsilon_{\mathrm{xx}}(\delta x_{\mathrm{n}} - \delta x_{\mathrm{f}})$	$(\delta x_{\mathrm{n}} - \delta x_{\mathrm{f}})\varepsilon_{\mathrm{xx}} < 4.5\ \mu\mathrm{m}$
5	$15 k_{\mathrm{eff}} T^4 T_{\mathrm{xx}} \Omega_{\mathrm{or}} \left(\frac{k_{\mathrm{eff}}\hbar}{Lm} + 9T\Omega_{\mathrm{or}}^2\right)(\delta z_{\mathrm{f}} - \delta z_{\mathrm{n}})$	$(0.84\ \mathrm{m}^{-1})(\delta z_{\mathrm{f}} - \delta z_{\mathrm{n}})$	$(\delta z_{\mathrm{f}} - \delta z_{\mathrm{n}}) < 120\ \mu\mathrm{m}$
6	$30 k_{\mathrm{eff}} T^4 \Omega_{\mathrm{or}}^3 \left(\frac{k_{\mathrm{eff}}\hbar}{Lm} + 9T\Omega_{\mathrm{or}}^2\right) \varepsilon_{zz}(\delta z_{\mathrm{f}} - \delta z_{\mathrm{n}})$	$(1.7\ \mathrm{m}^{-1})\varepsilon_{zz}(\delta z_{\mathrm{f}} - \delta z_{\mathrm{n}})$	$\varepsilon_{zz} < 0.49$
7	$\frac{45}{2} k_{\mathrm{eff}} T^5 \left(T_{\mathrm{xx}}^2 + 6T_{\mathrm{xx}}\Omega_{\mathrm{or}}^2 + 4T_{zz}\Omega_{\mathrm{or}}^2 + 5\Omega_{\mathrm{or}}^4\right) \Delta v_x$	$(270\ \mathrm{s/m})\Delta v_x$	$\Delta v_x < 370\ \mathrm{nm/s}$
8	$3 k_{\mathrm{eff}} T^4 \Omega_{\mathrm{or}} \left(\frac{9 k_{\mathrm{eff}}^2 \hbar^2}{L^2 m^2} - 5T_{\mathrm{xx}}\right) \Delta v_z$	$(9.6 \times 10^3\ \mathrm{s/m})\, \Delta v_z$	$\Delta v_z < 10\ \mathrm{nm/s}$
9	$30 k_{\mathrm{eff}} T^4 \varepsilon_{zz} \Omega_{\mathrm{or}}^3 \Delta v_z$	$(1.9 \times 10^4\ \mathrm{s/m})\, \varepsilon_{zz} \Delta v_z$	$\varepsilon_{zz} < 0.52$
10	$60 \frac{\hbar k_{\mathrm{eff}}^2}{L^2 m} T^4 T_{\mathrm{yy}} \delta v_{\mathrm{yn}} \delta y_{\mathrm{n}}$	$(4.3 \times 10^{-2}\ \mathrm{s/m^2})\, \delta v_{\mathrm{yn}} \delta y_{\mathrm{n}}$	$\delta v_{\mathrm{yn}} \delta y_{\mathrm{n}} < 23\ \mathrm{cm^2/s}$
11	$36 k_{\mathrm{eff}}^3 \frac{\hbar^2}{Lm^2} \Omega_{\mathrm{or}} T^3 (7 + 8\cos(\omega T)) \sin^4\left(\frac{\omega T}{2}\right) \overline{\delta\theta}$	$(3.9 \times 10^5)\, \overline{\delta\theta}$	$\overline{\delta\theta} < 0.26\ \mathrm{nrad}$
12	$4 k_{\mathrm{eff}} \delta z_n (7 + 8\cos(\omega T)) \sin^4\left(\frac{\omega T}{2}\right) \overline{\delta\theta}$	$(1.3 \times 10^{10}\ \mathrm{m}^{-1})\, \delta z_n \overline{\delta\theta}$	$\overline{\delta\theta} < 0.77\ \mathrm{nrad}$
13	$\frac{27\sqrt{2}}{4} k_{\mathrm{eff}} x_n \frac{L}{R} \Omega_{\mathrm{or}}^2 T^2 \chi(\omega T) \overline{\delta\theta}$	$(1.1 \times 10^4)\, x_n \overline{\delta\theta}$	$\overline{\delta\theta} < 0.91\ \mathrm{nrad}$

J. Hogan et al., GRG **43**, 7 (2011).

Wavefront distortion: temporal variations

Time varying wavefront inhomogeneities will lead to non-common phase shifts between distant clouds of atoms

- High spatial frequencies diffract out of the laser beam as the beam propagates between atom clouds

- Limit for temporal stability of wavefronts determined by stability of final telescope mirror

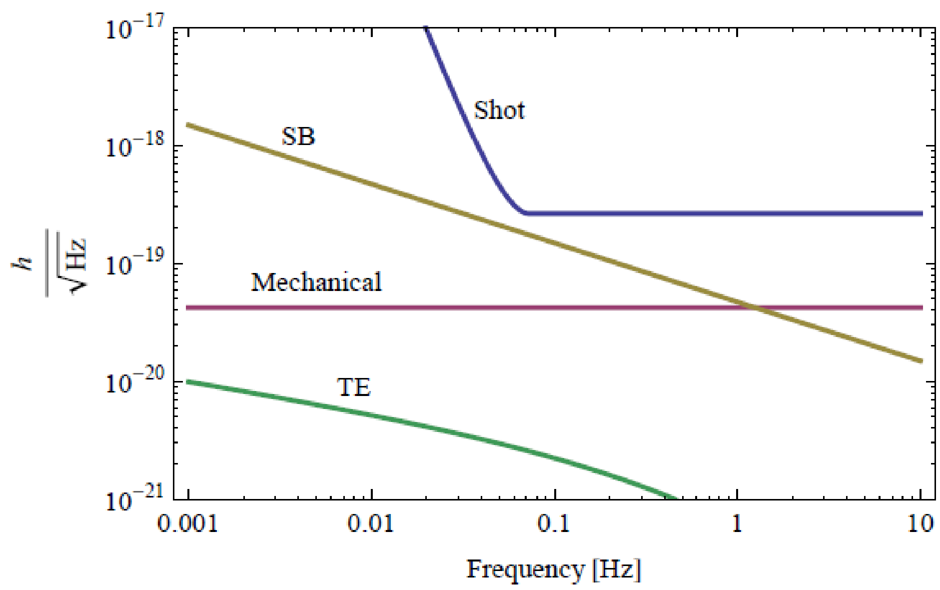

Mirror: Be at 300K

J. M. Hogan, *et al.*, arXiv 1009.2702 (2010), GRG (2011).

See also, P. Bender, PRD (2011) and Hogan, PRD (2011).

Atom cloud kinematic constraints

Shot-to-shot jitter in the position of the atom cloud with respect to the satellite/laser beams constrains static wavefront curvature

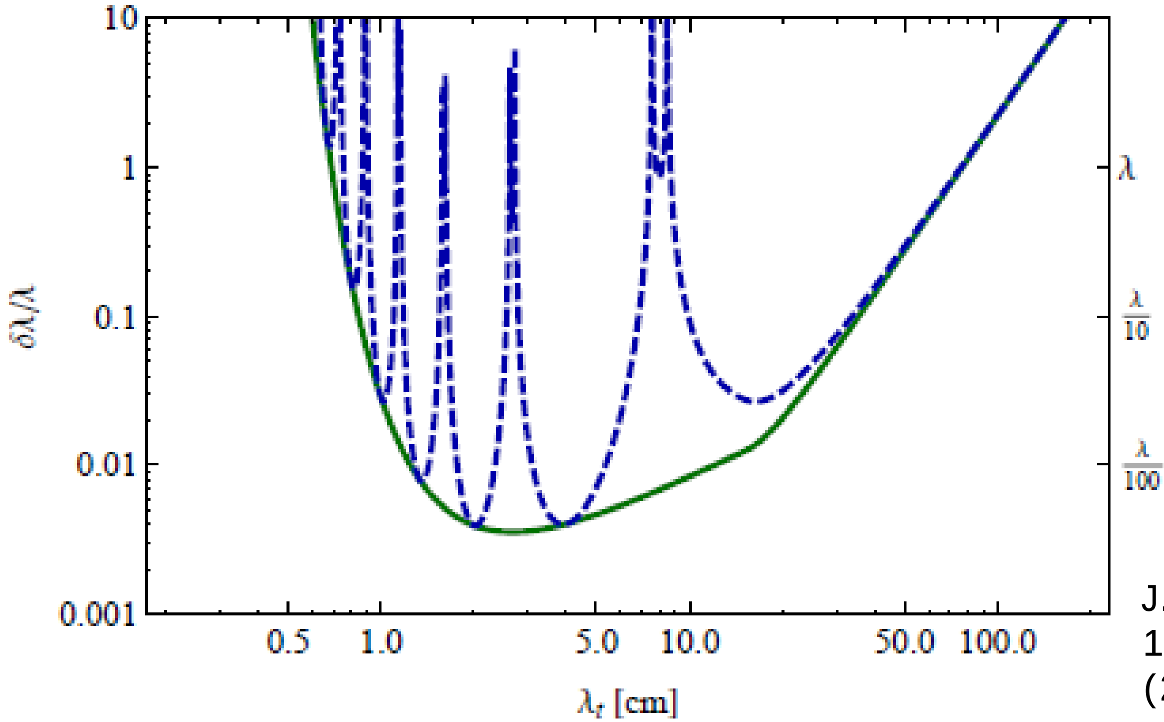

Wavefront error vs. spatial frequency, assuming 10 nm/Hz$^{1/2}$ position jitter

J. M. Hogan, *et al.*, arXiv, 1009.2702 (2010), GRG (2011).

Two-photon vs. Single photon configurations

2-photon transitions

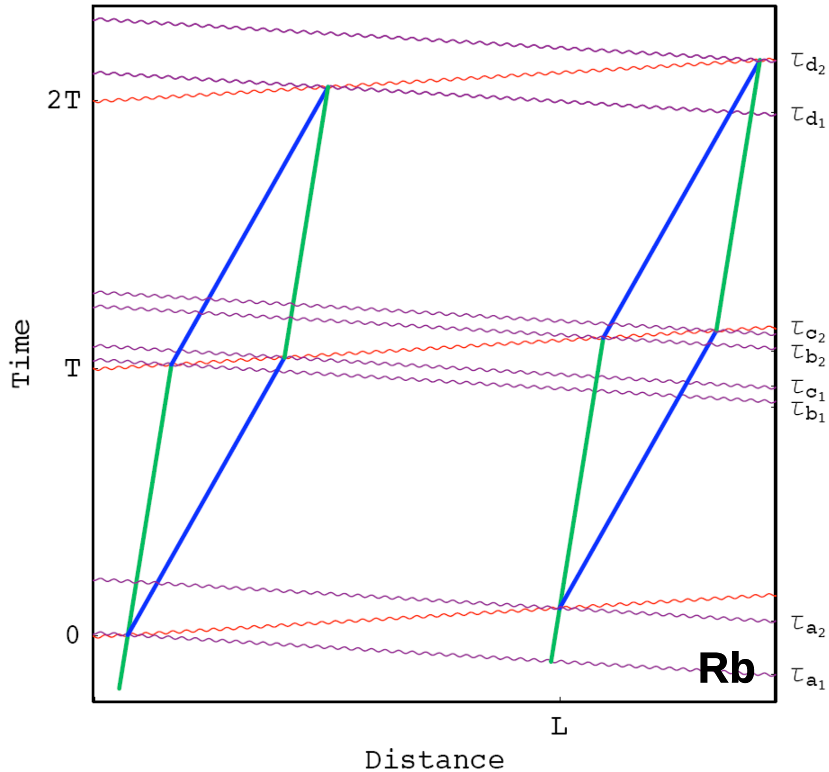

GW signal from relative positions of atom ensembles with respect to optical phase fronts.

1 photon transitions

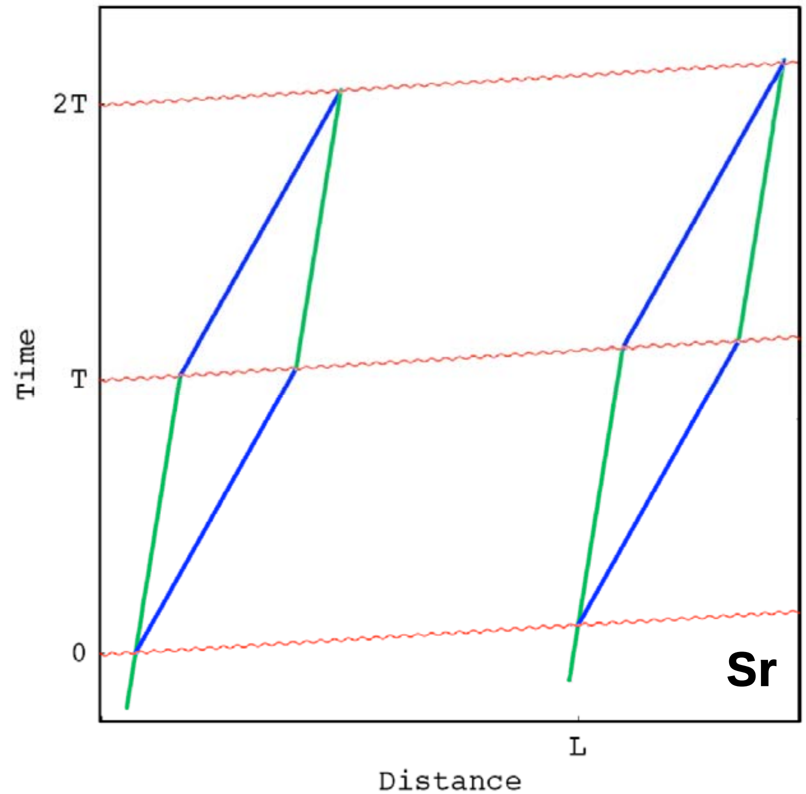

GW signal from light propagation time between atom ensembles.

Dimopoulos, et al., PRD (2008)

Laser frequency noise insensitive detector

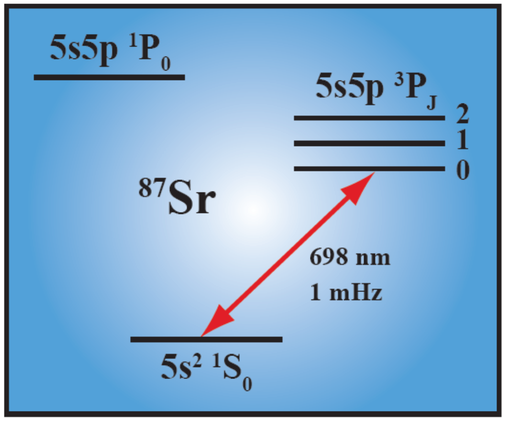

Clock transition in candidate atom ^{87}Sr

- Long-lived single photon transitions (e.g. clock transition in Sr, Ca, Yb, Hg, etc.).
- Atoms act as clocks, measuring the light travel time across the baseline.
- GWs modulate the laser ranging distance.

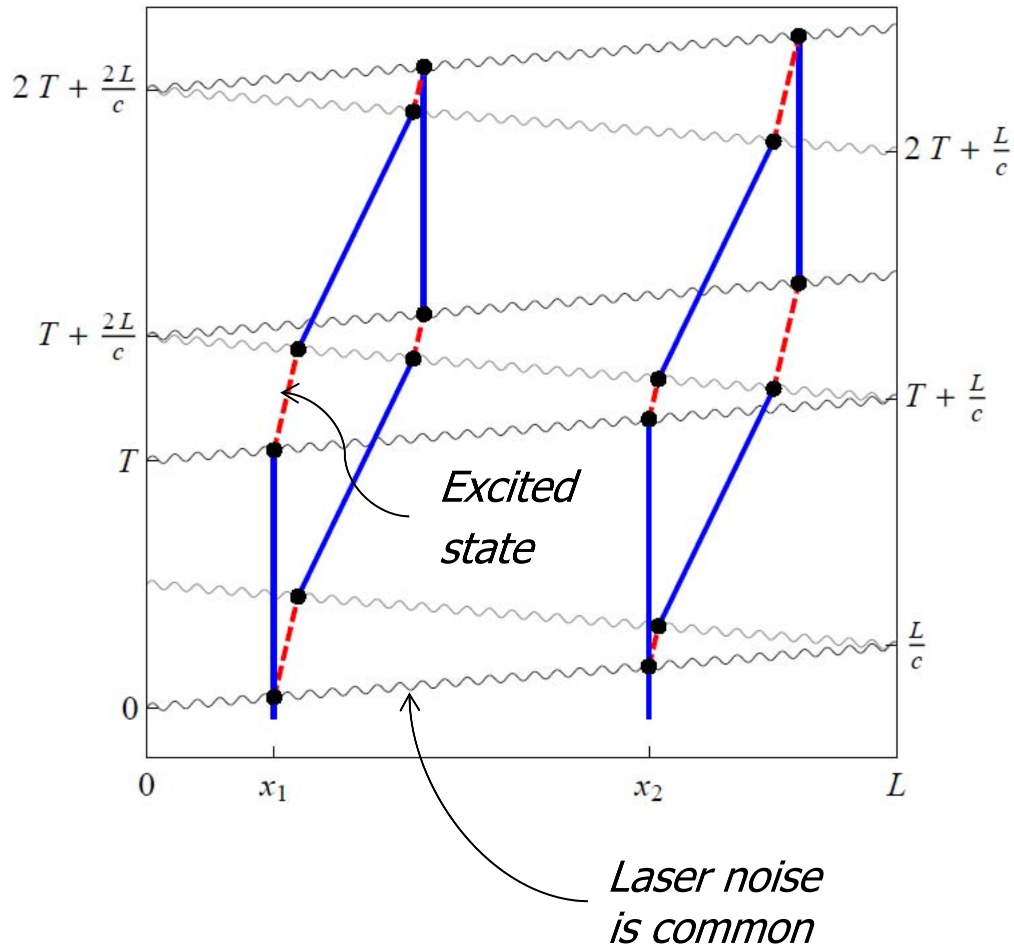

Graham, *et al.*, arXiv:1206.0818, PRL (2013)

2 Satellite Sr Single Photon

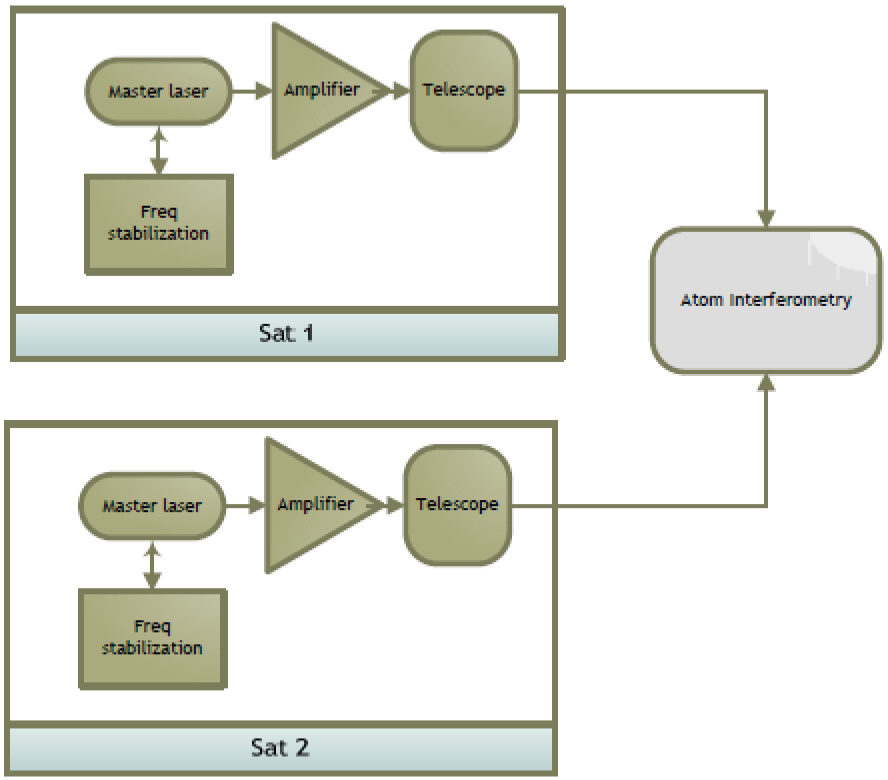

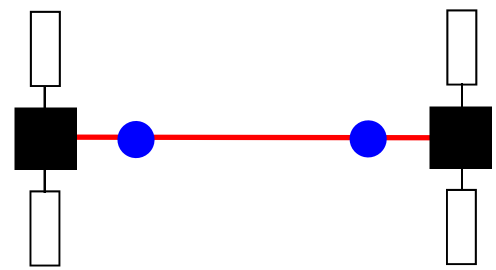

- Single baseline (two satellites)
- Single photon atom optics (e.g., Sr) for laser and satellite acceleration noise immunity
- Atoms act as clocks, measuring the light travel time across the baseline

Requirements for h = 1e-20/Hz$^{1/2}$

Attribute	**Req.**
Sat. acceleration noise (longitudinal)	10^{-8} g/Hz$^{1/2}$
Transverse position jitter	10 nm/Hz$^{1/2}$
Spatial wavefront	$\lambda/100$
Atom cloud temperature	1 pK
Pointing stability	0.1 μrad
Magnetic fields	4 nT/Hz$^{1/2}$
Laser phase noise	10 Hz linewidth; 100 kHz/Hz$^{1/2}$
Atom optics	100 $\hbar$k
Formation flying	2 satellites
Atom source	10^8/s Sr

Risk

Noise source	Risk
Magnetic Fields	Low
AC Stark	Low
Laser intensity jitter	Low
Atom source velocity jitter	Mid
Laser pointing jitter	Mid
Solar radiation	Low
Blackbody	Low
Atom flux	Low
Laser wavefront noise	High?
Atom detection noise	High?
Gravity gradient	Mid

See analysis in Graham, *et al.*, arXiv:1206.0818, PRL (2013) (and references therein).

DARPA QuASAR SBOC-1/Optical clock

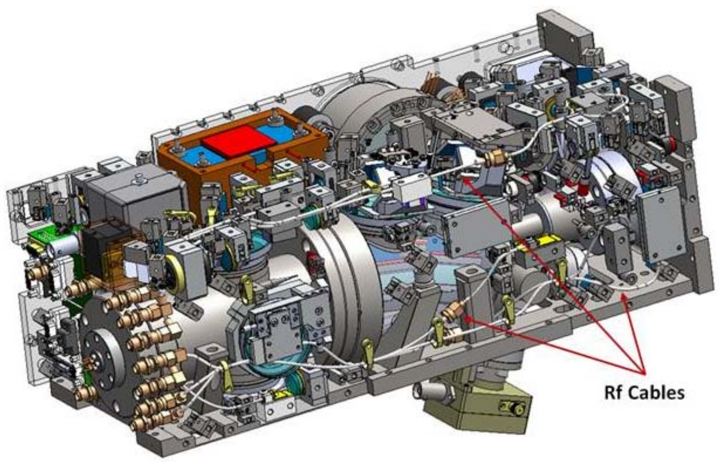

6 liter physics package.

Contains all lasers, Sr source, 2D MOT, Zeeman slower, spectrometer, pumps, and 3 W Sr oven; 4e10 cold a/sec.

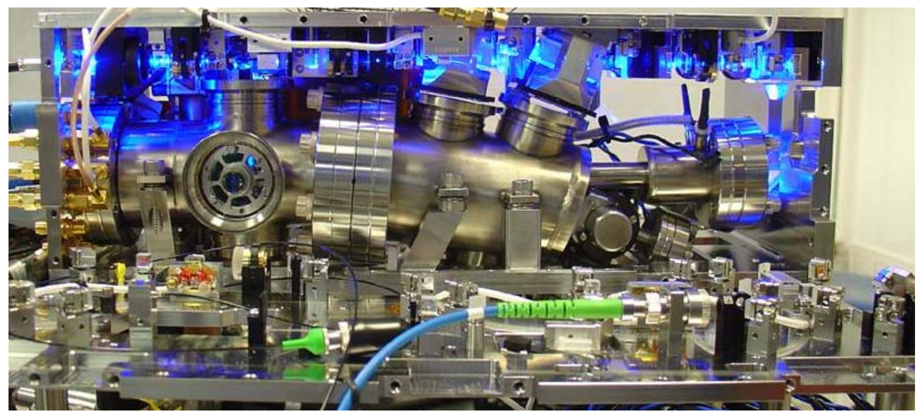

As built view with front panel removed in order to view interior.

AOSense

408-735-9500
AOSense.com
Sunnyvale, CA

Collaborators

Stanford University

PI:
Mark Kasevich

EP:
Susannah Dickerson
Alex Sugarbaker

LMT:
Sheng-wey Chiow
Tim Kovachy

Theory:
Peter Graham
Savas Dimopoulos
Surjeet Rajendran

Former members:
David Johnson (Draper)
Jan Rudolf (Rasel Group)

Also
Philippe Bouyer (CNRS)

NASA Goddard Space Flight Center

Babak Saif
Bernard D. Seery
Lee Feinberg
Ritva Keski-Kuha

AOSense